



**HAL**  
open science

## Using gold nanoparticles for enhanced intradermal delivery of poorly soluble auto-antigenic peptides

R K Singh, C. Malosse, J. Davies, Bernard Malissen, E. Kochba, Y. Levin, J C Birchall, S A Coulman, J Mous, M A Mcateer

### ► To cite this version:

R K Singh, C. Malosse, J. Davies, Bernard Malissen, E. Kochba, et al.. Using gold nanoparticles for enhanced intradermal delivery of poorly soluble auto-antigenic peptides. *Nanomedicine: Nanotechnology, Biology and Medicine*, 2020, 10.1016/j.nano.2020.102321 . hal-03013467

**HAL Id: hal-03013467**

**<https://hal.science/hal-03013467v1>**

Submitted on 23 Nov 2020

**HAL** is a multi-disciplinary open access archive for the deposit and dissemination of scientific research documents, whether they are published or not. The documents may come from teaching and research institutions in France or abroad, or from public or private research centers.

L'archive ouverte pluridisciplinaire **HAL**, est destinée au dépôt et à la diffusion de documents scientifiques de niveau recherche, publiés ou non, émanant des établissements d'enseignement et de recherche français ou étrangers, des laboratoires publics ou privés.



ELSEVIER

Nanomedicine: Nanotechnology, Biology, and Medicine  
xx (xxxx) xxx



nanomedjournal.com

# Using gold nanoparticles for enhanced intradermal delivery of poorly soluble auto-antigenic peptides ☆☆☆☆☆

R.K Singh<sup>a,1</sup>, C. Malosse<sup>b</sup>, J. Davies<sup>a</sup>, B. Malissen<sup>b,c</sup>, E. Kochba<sup>d</sup>, Y. Levin<sup>d</sup>, J.C Birchall<sup>e</sup>, S.A Coulman<sup>e</sup>, J. Mous<sup>f,2</sup>, M.A McAteer<sup>f</sup>, C.M Dayan<sup>a,\*</sup>, S. Henri<sup>b</sup>, F.S Wong<sup>a</sup>

<sup>a</sup>Division of Infection & Immunity, School of Medicine, Cardiff University, Heath Park, Cardiff, UK

<sup>b</sup>Centre d'Immunologie de Marseille-Luminy, Aix Marseille Université, Inserm, CNRS, Marseille, France

<sup>c</sup>Centre d'Immunophénomique, Aix Marseille Université, INSERM, CNRS, Marseille, France

<sup>d</sup>NanoPass Technologies Ltd., Nes Ziona, Israel

<sup>e</sup>School of Pharmacy and Pharmaceutical Sciences, Cardiff University, UK

<sup>f</sup>Midatech Pharma PLC, Cardiff, UK

Revised 8 August 2020

## Abstract

Ultra-small 1-2 nm gold nanoparticles (NP) were conjugated with a poorly-soluble peptide auto-antigen, associated with type 1 diabetes, to modify the peptide pharmacokinetics, following its intradermal delivery. Peptide distribution was characterized, in vivo, after delivery using either conventional intradermal injection or a hollow microneedle device. The poorly-soluble peptide was effectively presented in distant lymph nodes (LN), spleen and draining LN when conjugated to the nanoparticles, whereas peptide alone was only presented in the draining LN. By contrast, nanoparticle conjugation to a highly-soluble peptide did not enhance in vivo distribution. Transfer of both free peptide and peptide-NPs from the skin to LN was reduced in mice lacking lymphoid homing receptor CCR7, suggesting that both are actively transported by migrating dendritic cells to LN. Collectively, these data demonstrate that intradermally administered ultra-small gold nanoparticles can widen the distribution of poorly-soluble auto-antigenic peptides to multiple lymphoid organs, thus enhancing their use as potential therapeutics.

© 2020 Published by Elsevier Inc.

**Key words:** Gold nanoparticles; Hydrophobic; Peptide; Intradermal; Microneedle; Autoantigen

Type 1 diabetes is an autoimmune disease characterized by the destruction of insulin-producing beta cells within the pancreas.<sup>1</sup> Insulin maintains blood glucose levels but is not a cure. Hence, we seek strategies to deliver antigen-specific immunotherapy to reduce immune-mediated beta cell damage.

The skin is an accessible route for therapeutic delivery. The rich network of antigen-presenting cells, including epidermal Langerhans and dermal dendritic cells (DCs) in skin, facilitates both immune activation and regulation, upon delivery of a therapeutic.<sup>2-5</sup> Microneedles (MNs) are a viable alternative to

conventional hypodermic needles for intradermal (ID) delivery, being both minimally invasive and relatively pain-free.<sup>6,7</sup> A variety of MNs exists, including the 600 µm hollow MNs (MicronJet600™), which have been used in this study and in the clinical setting to deliver insulin,<sup>8</sup> influenza vaccine,<sup>9,10</sup> zoster vaccine<sup>11</sup> and polio.<sup>12,13</sup> MicronJet600™ hollow MNs reproducibly and effectively deliver material into the dermal compartment, with a significant vaccine dose-sparing effect and improved immunogenicity, compared with intramuscular and subcutaneous delivery.<sup>14</sup>

☆ **Funding:** This work was part of the EE-ASI European research network (Collaborative Project) supported by the European Commission under the Health Cooperation Work Programme of the 7th Framework Programme (grant agreement no. 305305).

☆☆ **Conflicts of interest:** none

☆☆☆ **Prior presentation:** Some of this work was presented in abstract form at the Immunology of Diabetes Society meetings in Munich in 2015 and San Francisco in 2017

\*Corresponding author at: Division of Infection & Immunity, School of Medicine, Cardiff University, Heath Park, Cardiff, UK.

E-mail address: dayancm@cardiff.ac.uk. (C.M. Dayan).

<sup>1</sup> \*\*Present address Department of Oncology, University of Oxford, Oxford, UK

<sup>2</sup> Present address MRM Consulting GmbH, Switzerland.

<https://doi.org/10.1016/j.nano.2020.102321>

1549-9634/© 2020 Published by Elsevier Inc.

Nanoparticles (NPs) can be conjugated to multiple therapeutics, including peptides, as drug delivery agents. They can protect peptides from degradation, and can form a depot at the site of injection so enhancing antigen retention and uptake by DCs. Moreover, small carbohydrate-coated gold NPs also offer reduced toxicity<sup>15</sup> and bio-compatibility as well as exhibiting anti-inflammatory properties.<sup>16</sup> Furthermore, gold (Au) can be easily and covalently decorated on its surface by exploiting the strong soft-soft interaction between Au atoms and sulfur. Therefore, gold NPs represent a versatile nanoplatform for development of epitope-based vaccines.<sup>17</sup>

Recently, NPs have been used to prevent autoimmune diabetes in the non-obese diabetic (NOD) mouse model of diabetes by generating tolerogenic DCs and promoting T regulatory cell expansion to re-establish immune tolerance.<sup>18,19</sup> Although promising, both studies utilized systemic (intravenous or intraperitoneal) delivery systems, as well as large (>50 nm) NPs. In humans, skin-mediated delivery is more practical and convenient, has fewer safety concerns and can exploit the local immune cells. We have recently demonstrated that gold NPs (Midacore™) (<5 nm hydrodynamic radius), conjugated to a peptide autoantigen, can be effectively delivered into the dermal and epidermal layers of human skin explants by MicronJet600™ hollow MNs and target local antigen-presenting cells.<sup>20</sup> This present study is the first published report exploring the in vivo pharmacokinetics and resulting systemic immune response following MN-mediated delivery of a poorly-soluble auto-antigenic peptide conjugated to ultra-small gold NPs.

## Methods

### Animal models

BDC2.5 TCR transgenic NOD mice<sup>21</sup> have diabetogenic CD4+ T-cells that recognize a hybrid insulin-chromogranin A peptide (HIP)<sup>22</sup> and mimotope peptides (the specific one used in this study is designated BDC2.5mimotope peptide).<sup>23</sup> The mice were purchased from the Jackson laboratory and have been bred in a specific pathogen-free facility of Cardiff University. OTII TCR transgenic C57BL/6J mice<sup>24</sup> and CCR7<sup>-/-</sup> mice<sup>25</sup> on the C57BL/6J genetic background have previously been described. C57BL/6J mice were purchased from Janvier (France). Mice were maintained in individually-ventilated filter cages in scintainers on a 12 h light/dark cycle. Animal procedures were approved by University ethical review committee. All procedures relating to NOD mice were performed in accordance with protocols approved by the UK Home Office. All procedures relating to OTII and CCR7<sup>-/-</sup> mice were carried out in accordance with French and European directives.

### Peptides and solubility

The peptides (physicochemical properties shown in Table 1) were purchased from Peptide Synthetics, manufactured to >95% purity: BDC2.5mimotope – YVRPLWVRME; Hybrid Insulin Peptide (HIP) – DLQTLALWSRMD; Ovalbumin323-339 peptide (OTII)-ISQAVHAAHAEINEAGR.

### NP synthesis/characterization

Gold NPs (Midacore™) with a gold core size of <5 nm were synthesized and supplied by Midatech Pharma.<sup>20</sup> NPs were conjugated with each of the poorly-soluble HIP and BDC2.5mimotope peptides as well as the highly-soluble ovalbumin peptide, OTII, using custom-synthesized peptides with a thiol propionic acid linker, in an amide linkage at the N terminal (–S(CH<sub>2</sub>)<sub>2</sub>–CONH) (AmbioPharm Inc., North Augusta, SC, USA). Figure 1 illustrates the schematic structure of NPs covalently linked to BDC2.5mimotope peptide and Table 2 summarizes the NP properties. For all reactions, gold (III) chloride was mixed with a 3-fold excess of organic ligands and peptide in different ratios (5% β glucose C2 (synthesized in-house) and either 94% or 92% L-glutathione oxidized (Sigma Aldrich) and 1% or 3% peptide). Glutathione enabled non-enzymatic intracellular activation and release. The NPs were produced by reduction, following rapid addition of a 20-fold molar excess, relative to gold, of freshly-made 1 M sodium borohydride (Sigma Aldrich, Poole, UK) under vigorous vortex mixing. The samples were continuously vortexed for 1 min followed by a further 1 h constant mixing on a flatbed shaker at room temperature. After 1 h, the NP samples were concentrated by ultrafiltration using Amicon Ultra-15 centrifugal filter tubes (Millipore Ltd., 10 K membrane molecular weight cut-off) and washed 4 times with Milli-Q water (4 ml) to remove unbound peptide and residual borohydride.

The NP gold content was determined using a colorimetric gold assay. Hydrodynamic size and zeta potential of the NPs in water/10% PBS were determined by dynamic light scattering (DLS) using a Zetasizer Nano ZSP (Malvern instruments). Peptide content of the NP samples was determined by HPLC using a Varian 900-LC, with a reverse phase C18 column (Acquisition time: 11.2 min; Temperature = 35 °C; Slit width = 2 nm; 95% water, 5% acetonitrile gradient (1 ml/min) switching at 8 min, switch to 20% water, 80% acetonitrile). In brief, an aliquot of NPs (10 μl) was mixed with 40 μl of KCN solution (100 mM in 10 mM potassium hydroxide) to dissolve the gold. The sample was analyzed by HPLC at 212 nm to determine released peptide concentration, and at 400 nm to confirm that all the gold was dissolved. An aliquot of NPs (10 μl), diluted with 20 μl TFA, was also analyzed by HPLC to determine whether any free peptide remained in the NP solution, following ultrafiltration purification.

### ID injection of peptide-loaded NPs

Mice were anesthetized using isoflurane and the injection site was shaved prior to delivery. Free peptide or peptide-loaded NPs were injected intradermally in 50 μl sterile PBS using a 29G needle.

### MN characterization and injection of peptide-loaded NPs

Hollow MN devices (MicronJet600™) were provided by NanoPass Technologies. MicronJet is a CE marked and FDA cleared device, consisting of three MNs, each 600 μm in length, with a lumen of approximately 60 μm in diameter, bonded to a plastic adapter that attaches to a Luer syringe.<sup>14</sup> MicronJet600™

t1.1 Table 1

t1.2 Physicochemical properties of peptides used, listed in order of hydrophobicity with BDC2.5 being the most hydrophobic and OVA being the least hydrophobic (genscript online resource, available at <https://www.genscript.com/ssl-bin/site2/peptidecalculation.cgi>).

t1.3	Peptide	Sequence	Charge	Isoelectric point	pH	% hydrophobic/hydrophilic residues
t1.4	BDC2.5	YVRPLWVRME	1	9.34	Basic	Hydrophobic: 60% Hydrophilic: 10% Neutral: 30%
t1.5	HIP	DLQTLALWSRMD	-1	4.11	Acidic	Hydrophobic: 50% Hydrophilic: 25% Neutral: 25%
t1.6	OTII	ISQAVHAAHAEINEAGR	1	6.5	Basic	Hydrophobic: 47.1% Hydrophilic: 23.5% Neutral: 29.4%

162 injection did not change the diameter of NPs, which remained  
 163 physically stable under the shear forces of the injection.<sup>26</sup> Mice  
 164 were anesthetized using isoflurane, the injection site was shaved,  
 165 and peptide was injected in 50  $\mu$ l sterile PBS.

#### 166 Adoptive cell transfer

167 Splenic BDC2.5 CD4<sup>+</sup> T-cells were purified using a MACS  
 168 CD4 II negative selection kit (Miltenyi Biotec). Cells were  
 169 labeled with 20  $\mu$ M CFDA (Invitrogen) in 10% fetal calf serum  
 170 (FCS) RPMI at room temperature for 5 min at a concentration of  
 171  $10^7$ /ml. The cells were then washed twice in RPMI containing  
 172 FCS, rested for 15 min, and subsequently washed in saline.  
 173 These cells were then re-suspended at  $4 \times 10^6$  cells in 200  $\mu$ l  
 174 sterile saline and injected intravenously into 6-10-week-old  
 175 female mice. At the indicated times, single-cell suspensions were  
 176 prepared from spleen and various LNs, and CD4<sup>+</sup> T-cells were  
 177 analyzed by FACS. OTII T-cells were isolated from pooled LNs  
 178 and spleen of OTII mice, maintained on a *Rag-2*<sup>-/-</sup>xB6  
 179 [CD45.1] background, using a CD4<sup>+</sup> T-cell negative isolation  
 180 kit (Dynal, Invitrogen). For CTV labeling, purified OTII T-cells  
 181 were resuspended in PBS containing 2.5 mM cell tracer violet  
 182 (CTV) (Molecular Probes) for 3 min at room temperature.  $10^6$

CTV-labeled OTII T-cells were adoptively transferred into the 183  
 specified mice. 184

#### Phenotypic analysis by flow cytometry 185

All antibodies were purchased from BioLegend and BD 186  
 Pharmingen. 187

A single cell suspension was pre-treated with anti-CD16/32 188  
 (BD Pharmingen) and then stained at 4 °C for 25min with the 189  
 following pre-titrated mAbs against the indicated antigens: CD4- 190  
 AF700 (RM4-5), CD44-BV71 (IM7), CD3e-AF700 (500A2), 191  
 CD45.1-APC (A20), CD4-BV786 (RM4-5) and TCR V $\alpha$ 2-PE 192  
 (B20.1). To assess intracellular expression, samples were 193  
 permeabilized and fixed using Foxp3 transcription factor 194  
 staining buffer set (eBioscience), according to the manufacturer's 195  
 instructions. Intracellular mAbs against the following proteins 196  
 included: CTLA4-BV421 (UC10-4B9), IL10-BV650 (JES5- 197  
 16E3) and IFN $\gamma$ -PeCY7 (XMG-1.2). Cell viability was evalu- 198  
 ated using fixable viability dye efluor780 (eBioscience) or 199  
 zombie yellow (Biolegend), according to the manufacturer's 200  
 instructions. Samples were washed and read using a FACS 201  
 LSRII Fortessa cytometer with DIVA software (BD) and 202  
 analyzed using FlowJo software (TreeStar). 203

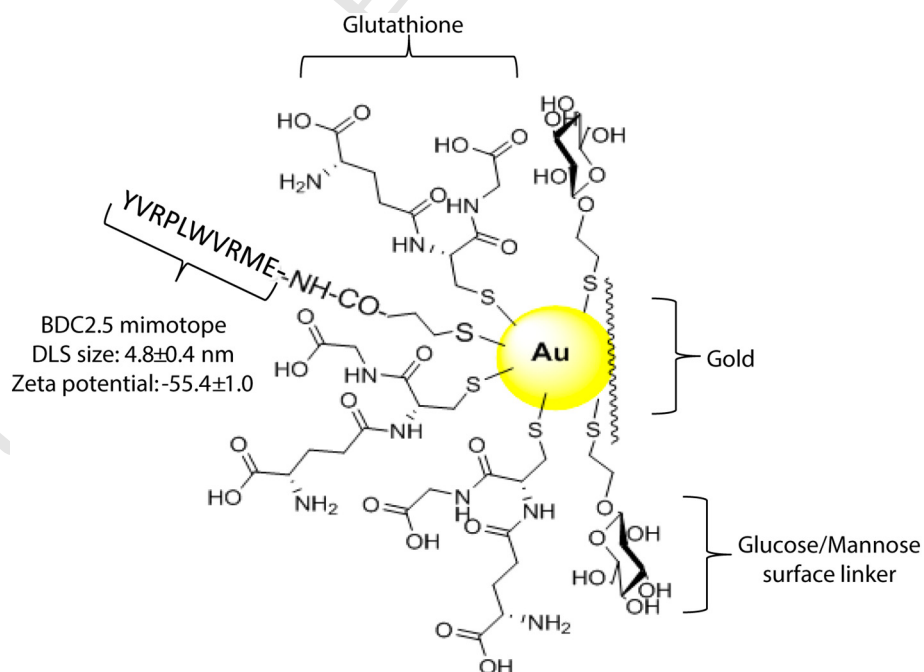


Figure 1. **Gold NP composition.** Composition of gold NPs used, comprising a gold core, conjugated via sulfur bonds to an organic layer of glucose or mannose, glutathione and peptide, (BDC2.5mimotope).

Peptide	DLS size (nm)	Zeta potential	Peptide loading levels
BDC2.5	4.8 ± 0.4	-55.4 ± 1.0	2%
HIP	3.3 ± 1.0	-54.7 ± 1.0	2%
OVA	6.3 ± 0.8	-45.3 ± 0.6	2%

## 204 Statistical analysis

205 All results are presented as the mean ± standard error of the  
 206 mean (SEM) and were analyzed using GraphPad Prism V5.  
 207 Student's *t* test, one-way ANOVA and two-way ANOVAs (for  
 208 analyses with more than 1 variable) with Bonferroni post-hoc test  
 209 were used for statistical analysis. *P* values of <0.05 were  
 210 considered statistically significant: \*denotes *P* < 0.05, \*\*de-  
 211 notes *P* < 0.01, \*\*\*denotes *P* < 0.001.

## 212 Results

### 213 Pharmacokinetics of intradermally-delivered BDC2.5mimotope 214 peptide coupled to NP differs from BDC2.5mimotope peptide 215 alone in vivo

216 Following the intravenous transfer of CFDA-labeled islet-  
 217 specific BDC2.5 CD4+ T-cells into naïve NOD mice,

BDC2.5mimotope NPs, BDC2.5mimotope peptide alone (2 µg 218  
 peptide in 50 µl) or peptide free 'blank' NPs were administered 219  
 by ID injection at the back of the neck. Lymphoid organs were 220  
 then analyzed at 24, 48 and 72 h. Following administration of 221  
 BDC2.5mimotope NPs, BDC2.5 T-cell proliferation in the skin- 222  
 draining LN (axillary), the non-draining LN (inguinal), the 223  
 spleen and pancreatic LN (PLN) was enhanced, compared to 224  
 baseline at the 48 and 72 h time points (Figure 2). In contrast, 225  
 levels of proliferation were much reduced in mice treated with 226  
 BDC2.5mimotope peptide alone; proliferation was only detected 227  
 in the axillary (draining) LN at the 72 h time point, with no 228  
 proliferation at either 24 or 48 h (and only baseline proliferation 229  
 in the PLN) (Figure 2). As expected, modest proliferation of 230  
 BDC2.5 CD4+ T-cells as a result of endogenous presentation of 231  
 the cognate antigen occurred in the pancreatic LN in control 232  
 mice. This was not enhanced following ID injection of peptide 233  
 and indicates that the peptide administered alone was not 234  
 disseminated to the PLN. No proliferation was observed using 235  
 peptide-free 'blank' NPs, confirming the antigen-specific nature 236  
 of the response. Overall, ID delivery of BDC2.5mimotope 237  
 peptide via NPs resulted in significantly higher levels of T-cell 238  
 proliferation in distant lymphoid tissues and at earlier time points 239  
 than peptide alone. 240

### 241 Peptide NP conjugation: the effects of T-cell affinity

242 CD4+ T-cells are central in the process of beta cell 242  
 243 destruction. BDC2.5 CD4+ T-cells are highly diabetogenic and 243

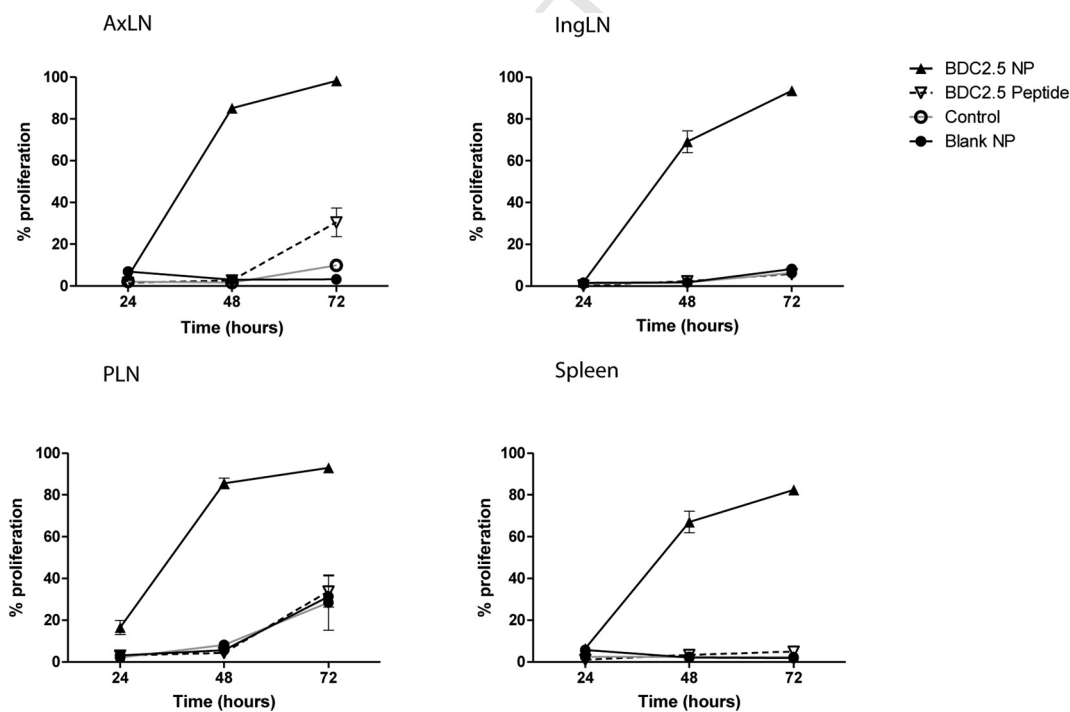
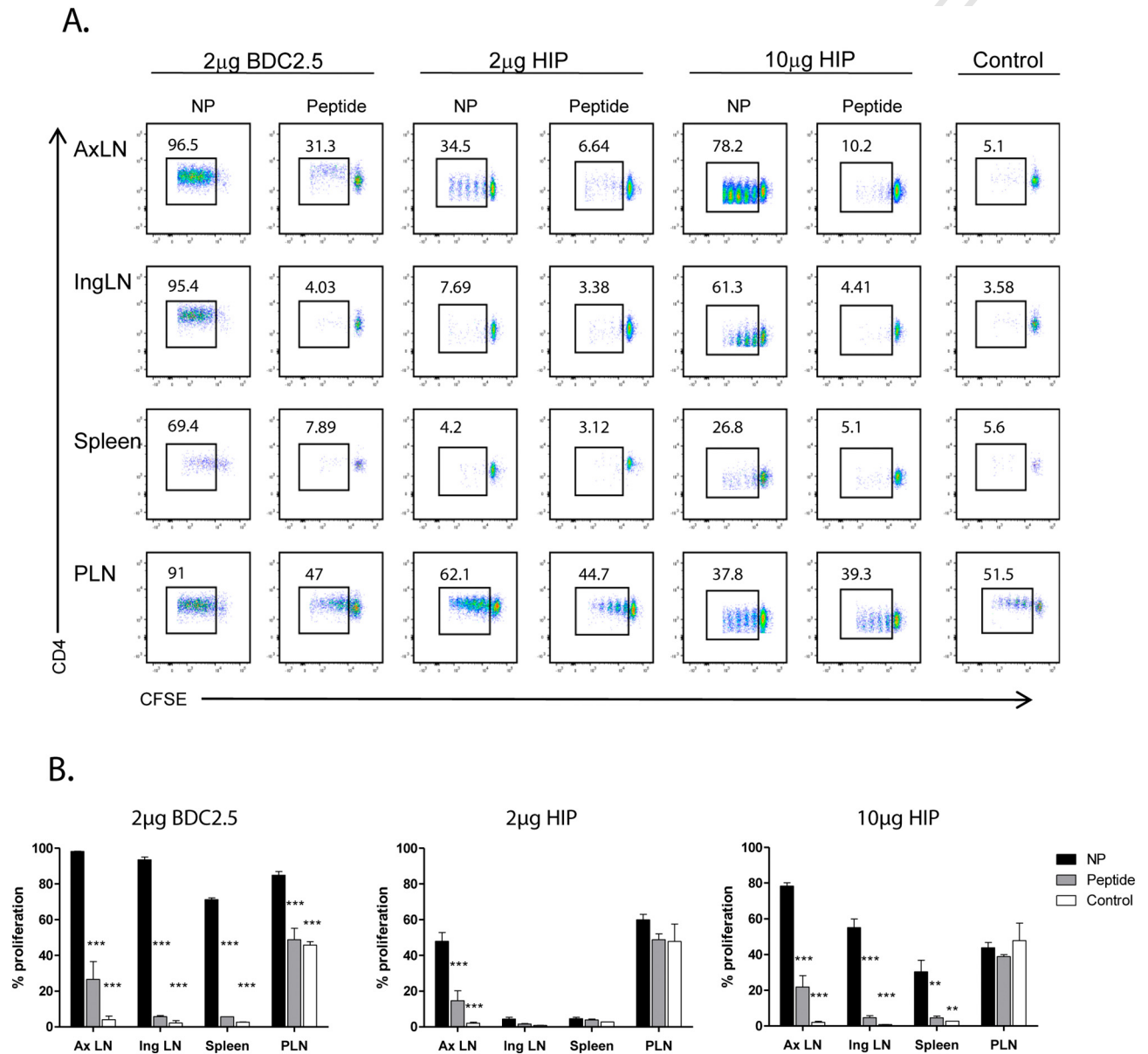


Figure 2. In vivo proliferation time course analysis following peptide-NP delivery compared to peptide alone. CFDA-labeled BDC2.5 CD4+ T-cells were transferred intravenously into NOD mice, followed by an ID injection of either 2 µg BDC2.5mimotope or BDC2.5mimotope-NP or peptide free 'blank' NP. Experimental control mice did not receive the ID injection. LNs (axillary, inguinal and pancreatic) and spleen were harvested at 24, 48 and 72 h following injection and BDC2.5 CD4+ T-cells analyzed for proliferation by CFSE dilution. Mean ± SEM with 3 mice per treatment is shown, representative of 3 experiments. Statistical analysis was done by two-way ANOVA with Bonferroni post-test comparing BDC2.5mimotope NP to BDC2.5mimotope peptide (\*\*\*) (*P* < 0.001).

244 the natural epitope for these pathogenic cells is a hybrid insulin  
 245 peptide (HIP), formed by the fusion of a chromogranin A peptide  
 246 sequence WE14 and insulin C-peptide.<sup>22</sup> Although naturally  
 247 formed, HIP has a lower affinity for BDC2.5 CD4<sup>+</sup> T-cells than  
 248 the commonly used high affinity islet antigenic peptide substitute  
 249 BDC2.5mimotope. Therefore, to determine whether NP conju-  
 250 gation changed these relative peptide affinities, NPs were  
 251 conjugated to either the high affinity BDC2.5mimotope peptide  
 252 or the lower affinity naturally-formed HIP peptide. CFDA-  
 253 labeled BDC2.5 CD4<sup>+</sup> T-cells were then intravenously trans-

ferred into NOD mice and these mice were subsequently treated 254  
 with an ID injection of an NP formulation (BDC2.5mimotope or 255  
 HIP peptide or peptide alone. At 72 h, proliferation of transferred 256  
 BDC2.5 CD4 T-cells was significantly higher in all lymphoid 257  
 tissues following treatment with the BDC2.5 NPs compared to 258  
 BDC2.5mimotope peptide (Figure 3, A and B), replicating 259  
 earlier findings shown in Figure 2. However, this effect was not 260  
 observed using the lower affinity HIP-NPs at an equivalent 261  
 peptide dose (2  $\mu$ g). Instead, HIP-NPs only induced proliferation 262  
 in the axillary LN and at lower levels than those seen with 263



**Figure 3. Peptide-NP effects on in vivo T-cell proliferation are dependent on peptide affinity.** CFDA-labeled BDC2.5 CD4<sup>+</sup> T-cells were transferred intravenously into NOD mice, followed by an ID injection of peptide or peptide-NP. LNs (axillary, inguinal and pancreatic) and spleen were harvested 72 h later and proliferation analyzed by flow cytometry. (A) Representative flow cytometric plots showing proliferative responses from left to right, 2  $\mu$ g BDC2.5mimotope-NP, 2  $\mu$ g BDC2.5mimotope peptide, 2  $\mu$ g HIP-NP, 2  $\mu$ g HIP peptide, 10  $\mu$ g HIP-NP, 10  $\mu$ g HIP peptide and no ID injection. (B) Left to right, summary of proliferation for high affinity BDC2.5mimotope and lower affinity 2  $\mu$ g and 10  $\mu$ g HIP epitope. Mean  $\pm$  SEM of 3 mice per treatment is shown, representative of 3 experiments. Statistical analysis was done using one-way ANOVA with Bonferroni post-test comparing peptide-NP to peptide and control (\*\* $P < 0.01$ , \*\*\* $P < 0.001$ ).

264 BDC2.5mimotope-NP, though still significantly higher than HIP  
 265 peptide alone. Endogenous proliferation in the pancreatic LN  
 266 was not enhanced by 2 µg HIP-NP. No proliferation above  
 267 control (no ID injection) was observed in the inguinal LN and  
 268 spleen. However, when a higher dose of HIP-NP was  
 269 administered (10 µg), widespread proliferation was observed in  
 270 these NP-treated mice, with profiles resembling those witnessed  
 271 with 2 µg BDC2.5mimotope NP. These results are consistent  
 272 with lower amounts of peptide-NP being present in distant LN  
 273 and in the case of a lower affinity peptide, may be limiting for T-  
 274 cell proliferation at lower doses. Dissemination of peptide alone  
 275 was much less efficient than its NP-formulated counterpart and  
 276 therefore no presentation was witnessed in the distant LNs, at  
 277 any of the doses of HIP peptide that were examined.

#### 278 *Peptide-NP conjugation: effects of peptide solubility*

279 The influence of peptide solubility on peptide-NP behavior  
 280 was also evaluated in vivo (Figure 4), by comparing the behavior  
 281 of the highly water-soluble OTII peptide, recognized by OTII  
 282 CD4+ T-cells, with the less soluble BDC2.5mimotope and HIP  
 283 peptide counterparts. CTV-labeled cells were transferred into  
 284 C57BL/6 mice, followed by OTII peptide or OTII-NP at 2 µg or  
 285 10 µg by ID injection, using 29G insulin needles. At a 2 µg OTII-  
 286 NP dose, T-cell proliferation occurred in all the lymphoid organs,  
 287 with greatest proliferation in the draining lymph nodes (brachial  
 288 and axillary LN). Moreover, at the higher dose of 10 µg, OTII-  
 289 NP induced significantly more T-cell proliferation than 2 µg  
 290 OTII-NP in the inguinal LN (\*\* $P < 0.01$ ) and spleen  
 291 (\*\* $P < 0.001$ ). In contrast to both BDC2.5mimotope and HIP  
 292 peptide, proliferation of T-cells in response to the OTII peptide  
 293 also reached almost 100%.

#### 294 *Peptide-NP can be successfully delivered via MicronJet600™* 295 *microneedles into murine skin*

296 To test whether using MicronJet600™ MNs would enhance  
 297 peptide-NP and free peptide delivery in vivo, experiments were  
 298 performed in both NOD and C57BL/6 mice. Following  
 299 intravenous transfer of BDC2.5 CD4+ T-cells into NOD mice  
 300 (Figure 5), and OTII cells into C57BL/6 mice (Figure 6), the  
 301 respective mice were injected with 2 µg BDC2.5mimotope-NP  
 302 or 2 µg OTII peptide-NP or soluble peptide using MicronJet  
 303 MNs. Lymphoid organs were harvested after 72 h and  
 304 proliferation was analyzed. Figures 5 and 6 indicate successful  
 305 peptide-NPs delivery using MNs, with high levels of prolifer-  
 306 ation in the skin-draining brachial and axillary LN, as well as the  
 307 inguinal LN and spleen, thus confirming the presentation of the  
 308 MN-delivered antigen to the responding T-cells. However, the  
 309 use of MicronJet needles, in this context, did not enhance  
 310 delivery of the BDC2.5mimotope peptide alone, nor alter the  
 311 delivery of OTII peptide compared to conventional ID injection.  
 312 Overall, proliferation following MN delivery was comparable to  
 313 that observed with conventional ID injection.

#### 314 *Peptide-NP is transported to LN by migratory skin DCs*

315 CCR7, a leukocyte chemotactic receptor, is expressed by  
 316 mature DCs and plays a key role in DC homing to LNs, as well as  
 317 their subsequent positioning within LN functional compart-

ments. Loss of CCR7 impedes DC migration from non-lymphoid 318  
 organs, such as the skin, into the draining LN.<sup>25,27</sup> With this in 319  
 mind, CCR7-deficient mice were used to determine the role of 320  
 DCs in distribution of OTII peptide and OTII peptide-NP, and to 321  
 determine whether peptide transport is an active DC-mediated 322  
 process. ID injection of OTII peptide and OTII-NP was therefore 323  
 examined at two different concentrations (2 µg and 10 µg) in wild 324  
 type C57BL/6 or CCR7KO C57BL/6 mice. A reduction in 325  
 proliferation was observed in different LN of the CCR7KO mice 326  
 following administration of the peptide-NP, with a significant 327  
 reduction at the higher 10 µg OTII concentration in both the 328  
 draining LN and spleen (\* $P < 0.05$ ) (Figure 7). Although the 329  
 same trend was observed with 2 µg OTII-NP and peptide alone, 330  
 the decrease was not statistically significant. This suggests that 331  
 migratory DCs are important for peptide-NP transport from the 332  
 skin to the draining LNs, particularly at high concentrations. 333

#### *HIP-NP influences cellular phenotype in a concentration-* *dependent manner* 334 335

To determine the impact of HIP-NP concentration on cell 336  
 function, NOD mice were transferred with CFDA-labeled 337  
 BDC2.5 CD4+ T-cells and then immediately treated with an 338  
 ID injection of 0.4 µg, 2 µg, 6 µg or 10 µg HIP-NP or free HIP 339  
 peptide. After 72 h, axillary draining LNs, the inguinal LN, 340  
 spleen and pancreatic LN were harvested and examined and a 341  
 concentration dependent HIP-NP proliferative response was 342  
 revealed. Proliferation in the axillary LN, inguinal LN and 343  
 spleen, was most notable at 10 µg. This was significantly higher 344  
 than the proliferation observed in the HIP peptide-administered 345  
 mice (Figure 8, A) and consistent with experiments that were 346  
 conducted with a more limited dose range (Figure 3). 347  
 Furthermore, the axillary LN T-cells expressed increased levels 348  
 of activation markers CD44 and CTLA4 (Figure 8, B), which 349  
 reached significance at lower concentrations compared with 350  
 proliferation in the inguinal LN and spleen. Despite enhanced 351  
 activation status, a significant decrease in cells expressing IFN $\gamma$  352  
 was noted in the axillary LN of HIP-NP treated mice compared to 353  
 peptide alone (\* $P < 0.05$ ). IL-10 expression was low under all 354  
 conditions (Figure 8, C). Therefore, while T-cells displayed an 355  
 increased activation and proliferation profile over a wide HIP-NP 356  
 range, functionally the cells of the draining LN produced less 357  
 IFN $\gamma$ . 358

#### 359 **Discussion**

The lipophilicity of 'naked' peptide autoantigens has been 360  
 shown to influence localized delivery in human skin<sup>28</sup>; results in 361  
 murine skin (Figures 2-6) provide further exemplification of this. 362  
 The murine dermis is an aqueous region, consisting of 60.3% 363  
 water,<sup>29</sup> and therefore the notable increase in T-cell proliferation 364  
 in response to intradermal administration of the water-soluble 365  
 OTII peptide (its cognate antigen) at lymphoid organs distant to 366  
 the local environment (Figure 7) is likely to be facilitated by 367  
 rapid diffusion in the local environment, uptake by DC in 368  
 draining LNs and subsequent distribution in the lymphatic 369  
 system. However more lipophilic auto-antigenic peptides such as 370  
 BDC2.5mimotope and HIP, which are insoluble in aqueous 371

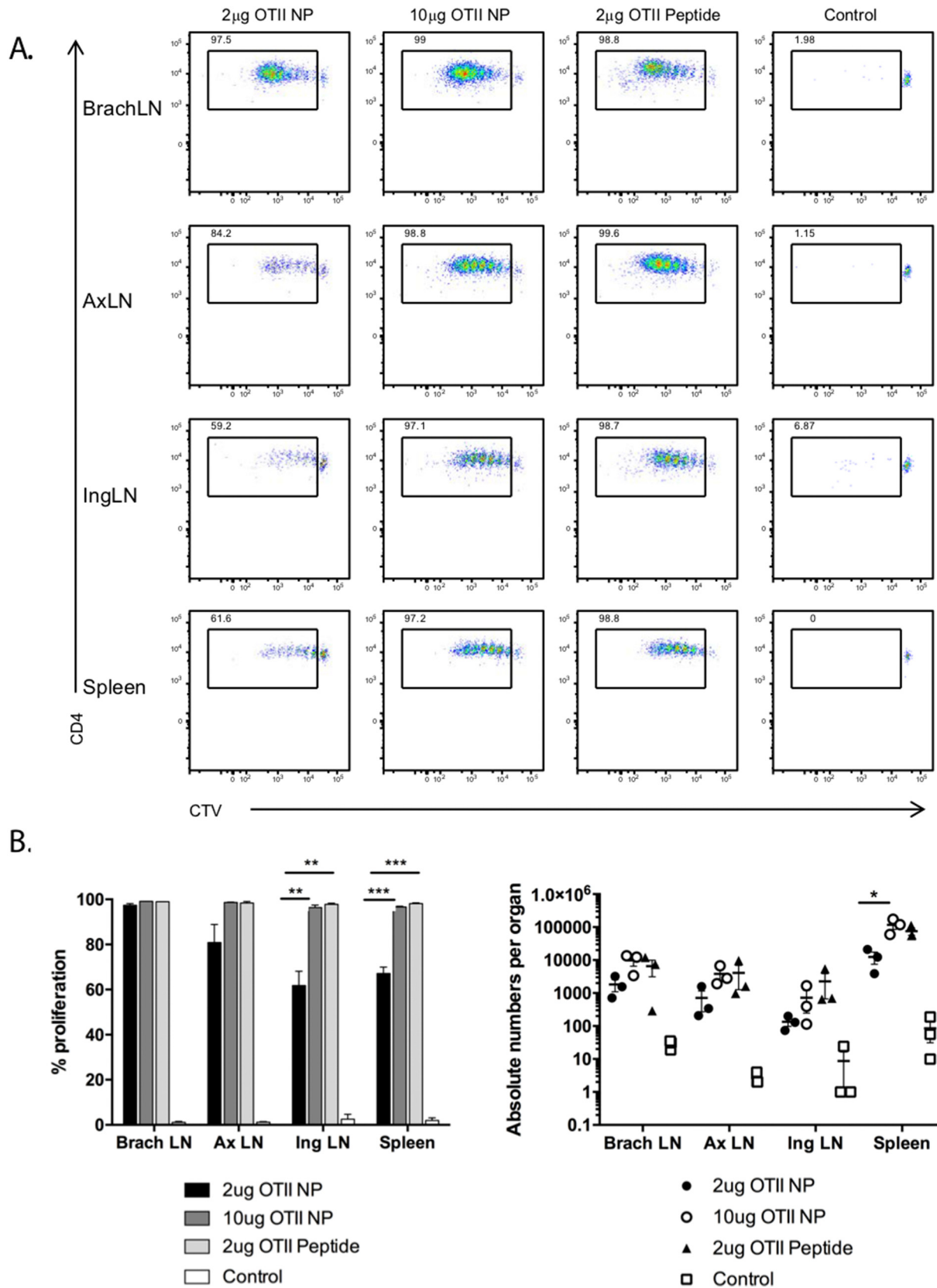
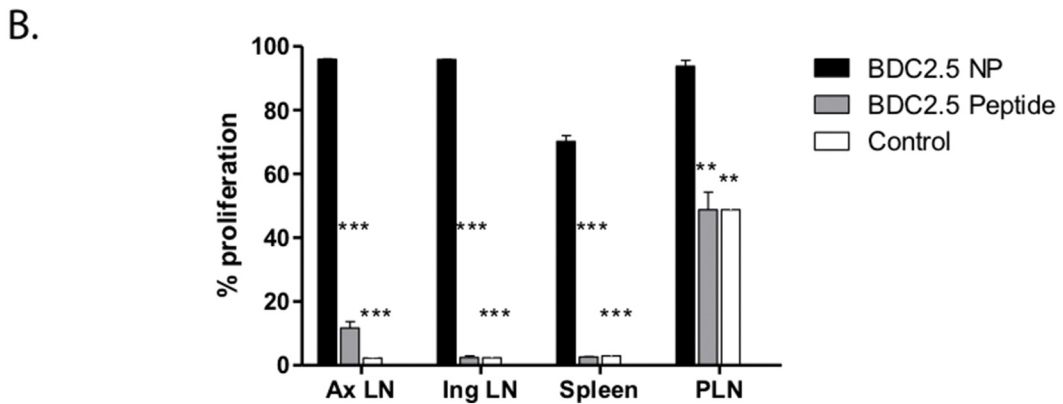
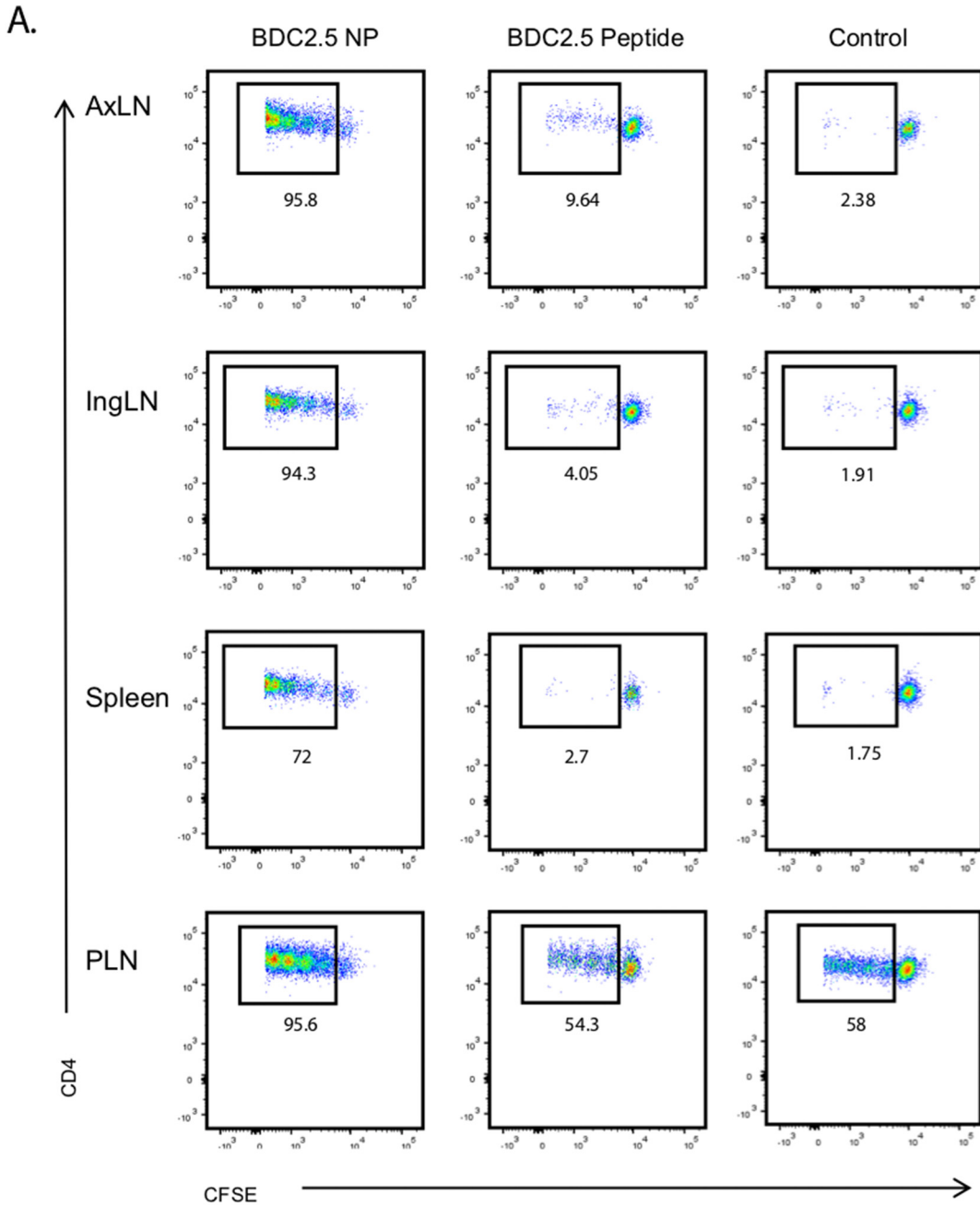
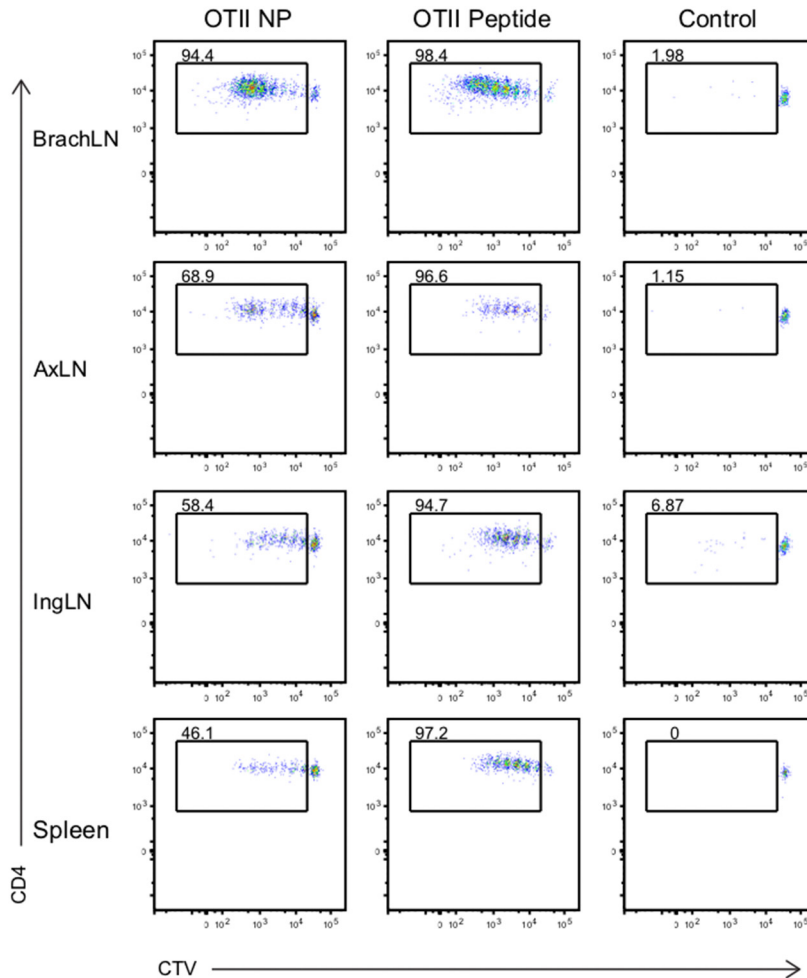


Figure 4. Peptide-NP effects in vivo differ according to peptide solubility. (A) Representative flow cytometric plots showing proliferative responses to (from left to right) 2 µg OTII-NP, 10 µg OTII-NP, 2 µg OTII peptide and controls in the brachial and axillary LNs (draining), distal inguinal lymph node and spleen. (B) Summary of proliferation for OTII-NP and peptide by % proliferation and absolute numbers. Data represent mean ± SEM (% proliferation) and each dot





A.



B.

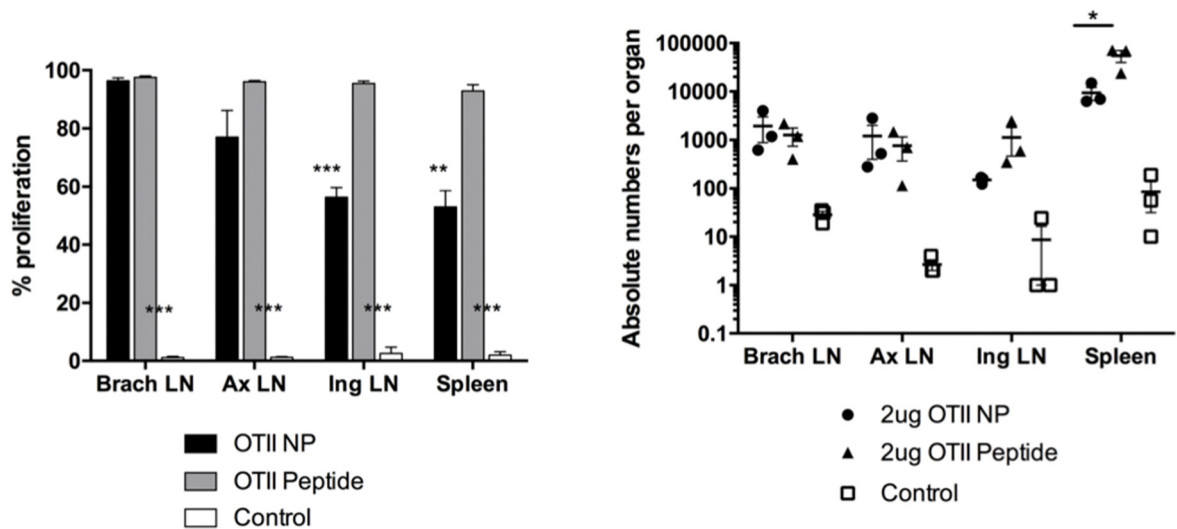


Figure 6. MicronJet600™ delivery of OTII peptide-NP and peptide alone induce proliferation of transferred T-cells. Mice received fluorescently-labeled cells intravenously, followed by an ID injection of peptide or peptide-NP using the short (600  $\mu$ m) hollow MN device (MicronJet600™). Lymph nodes were harvested 72 h later and proliferation was analyzed by flow cytometry. (A) Representative flow cytometric plots showing proliferative responses to 2  $\mu$ g OTII-NP, 2  $\mu$ g OTII peptide and controls in the brachial and axillary lymph nodes (draining), distal inguinal lymph node and spleen following MN delivery. (B) Summary of proliferation for OTII-NP and peptide. Mean  $\pm$  SEM (% proliferation) is shown and each dot corresponds to a mouse (absolute numbers per organ). Data are representative of three experiments with  $n = 2-3$  animals per group. Significant differences were identified using one-way ANOVA with Bonferroni post-test comparing peptide-NP to peptide and control (\*\* $P < 0.01$  \*\*\* $P < 0.001$ ).

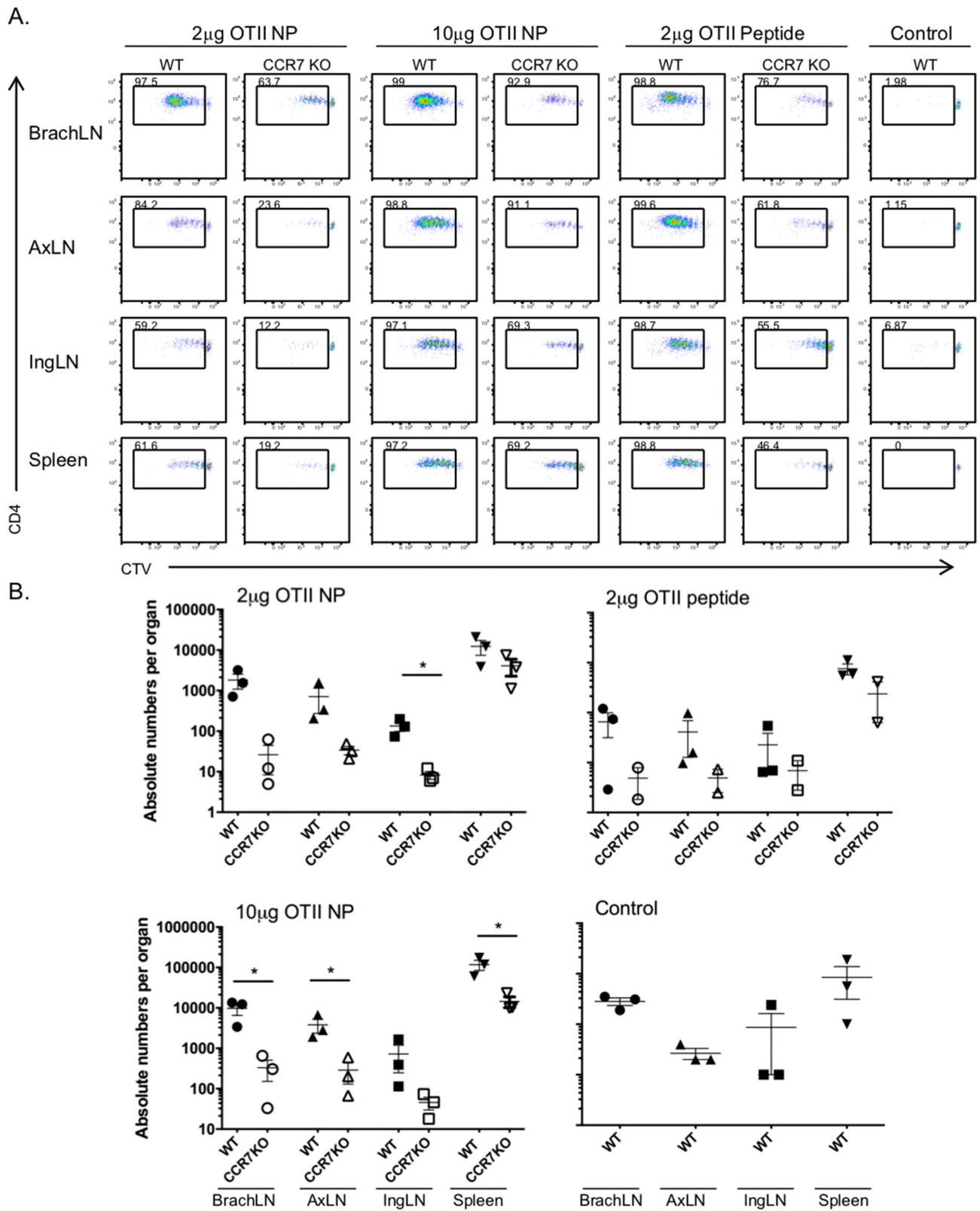
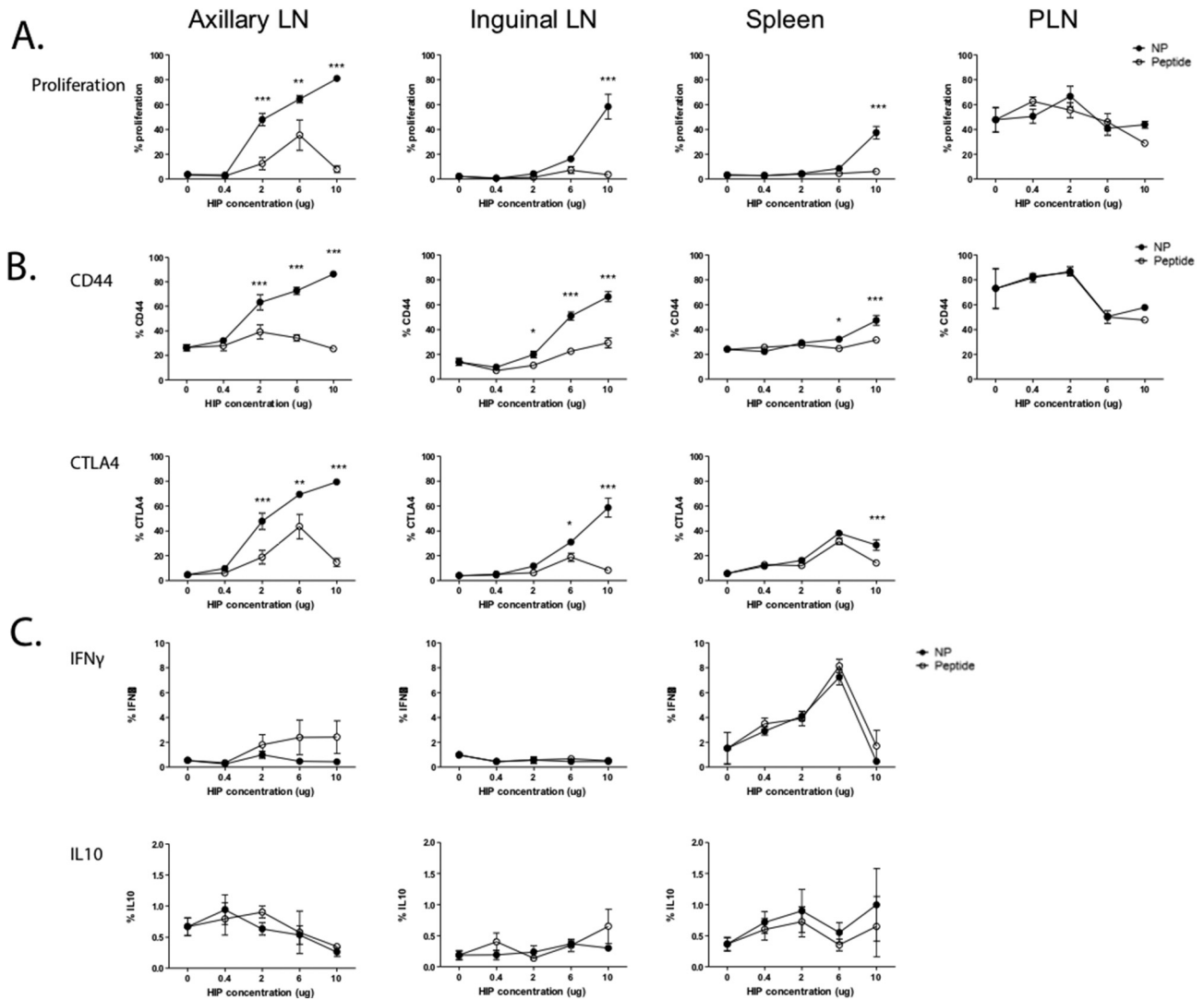


Figure 7. Peptide-NP is taken up by dendritic cells and distributed to lymphoid organs. WT and CCR7KO mice received CTV-labeled OTII T-cells intravenously, followed by an ID injection of peptide or peptide-NP using a 600 µm MicronJet600™ needle. LNs and spleen were harvested 72 h later and proliferation was analyzed by flow cytometry. (A) Representative flow cytometric plots showing proliferative responses (left to right) to 2 µg OTII-NP, 10 µg OTII-NP, 2 µg OTII peptide and controls in the brachial and axillary LN (draining), distal inguinal LN and spleen. (B) Absolute numbers of proliferating OTII CD4+ T-cells in response to OTII-NP and peptide. Each dot corresponds to a mouse and the mean (horizontal bar) is indicated. Data are representative of three



**Figure 8. HIP-NP has differential effects on the cellular phenotype dependent on concentration.** NOD mice received CFDA-labeled BDC2.5 CD4+ T-cells intravenously, followed immediately by an ID injection (29G insulin needle) of HIP-NP or HIP peptide at various concentrations. LNs were harvested 72 h later and CD4+ T-cells were analyzed by flow cytometry. (A) Proliferative response of cells to HIP-NP or peptide as determined by CFSE dilution. (B) BDC2.5 T-cell activation markers including CD44 and CTLA4 and (C) cytokine response including IFN $\gamma$  (axillary LN; interaction = ns, NP vs peptide  $p = *0.027$ , HIP concentration = ns) and IL10. Statistical analysis was done using two-way ANOVA with Bonferroni post-test comparing peptide-NP and peptide at individual concentrations (\* $P < 0.5$  \*\* $P < 0.01$ , \*\*\* $P < 0.001$ ). Mean  $\pm$  SEM is shown; data are representative of 3 experiments ( $n = 3$  per treatment).

372 media, such as water and PBS, are only able to stimulate  
 373 response in the local environment i.e. in the draining lymph node  
 374 (Figures 2-3). Enhancing the distribution of poorly water-soluble  
 375 peptides to stimulate immune responses distant from their  
 376 administration site may be desirable for a range of therapeutic  
 377 approaches, including immunotherapy for conditions such as  
 378 type 1 diabetes.

379 Gold NPs have recently garnered attention as drug delivery  
 380 agents for several reasons, including their lack of toxicity,<sup>31</sup>  
 381 chemical stability and extensive surface to volume ratio,<sup>32,33</sup>  
 382 which enable conjugation of clinically significant doses of  
 383 therapeutics. NPs have previously been used to deliver disease-  
 384 relevant autoantigens in mouse models of EAE,<sup>34–36</sup> arthritis<sup>37</sup>  
 385 ,<sup>38</sup> and diabetes.<sup>18,19,39</sup> Therefore, in this study we have  
 386 explored the potential of a gold NP formulation to enhance

trafficking of lipophilic peptides from the antigen-presenting cell  
 (APC) rich skin compartment to distant target sites, such as the  
 pancreas and pancreatic LN. We have also investigated the  
 importance of the mechanism of administration (microneedles  
 versus ID injection), peptide affinity, peptide solubility and  
 dosing on peptide-NP trafficking in vivo.

392 Peptide-NPs incorporating the relatively insoluble  
 393 BDC2.5mimotope and HIP peptides facilitated enhanced  
 394 proliferation at LNs distant to the site of intradermal injection,  
 395 thus indicating a marked improvement in distribution, in vivo,  
 396 compared to peptide alone. Enhanced proliferation of T-cells,  
 397 response to the NP-conjugated lipophilic peptides, was detectable  
 398 in the draining LN, the non-draining LN, the spleen and the  
 399 PLN, 48 h after intradermal administration. These kinetics are  
 400 consistent with a minimum requirement of 24 h for T-cell  
 401

proliferation to occur after antigen encounter. Conversely, conjugation of the highly water-soluble OTII peptide to the NP formulation reduced proliferation in the LNs at a “like for like” dose (2 µg) and it was only at an increased dose (10 µg) that the NP formulation performed comparably to the ‘naked’ peptide. This may be explained by a reduction in the diffusive properties of the hydrophilic peptide upon conjugation to a gold NP and, as a corollary, indicates that the enhancement afforded by conjugation of the lipophilic peptides to the ultra-small gold NPs may not be mediated simply by an increase in the solubility and diffusive properties of the therapeutic within the tissue. However, while these results are indicative, the lipophilic and hydrophilic peptides used in this study are detected by two different T-cell clones in two different mouse strains. Future experiments examining a range of peptide solubilities in a single mouse strain are therefore needed to probe this hypothesis further. Further studies could also explore whether NP-conjugation enhances peptide stability in vivo, as this may also contribute to enhanced and prolonged T-cell proliferation.

DCs are abundant in the immunocompetent skin. Increased peptide uptake by DCs in the local environment is more likely to result in increased activation and translocation of these highly effective APCs from the skin to the draining LNs and subsequent presentation to their cognate T-cells. Studies conducted in the CCR7-deficient mouse model at high OTII-NP concentrations (Figure 7) were therefore used to probe the role of DCs in trafficking locally-delivered NP-conjugated lipophilic peptides to distant LNs. Data indicate that distribution to LNs was partly dependent on DCs, with those mice lacking the lymph node homing receptor, CCR7, displaying reduced proliferation in response to peptide-NP administration (Figure 7). Previous studies suggest that intradermally-delivered antigens conjugated to a NP formulation diffuse within the extracellular environment to the draining LN for presentation to resident DCs in a size-dependent manner.<sup>5,42,43,45,46</sup> Furthermore, it has been hypothesized that ‘large’ NPs, ranging from 33 nm<sup>45</sup> to 500 nm,<sup>46</sup> are internalized by DCs at the site of injection and are trafficked to local LNs for presentation, while ‘small’ NPs are not retained in LNs, thereby reducing the magnitude and quality of the ensuing T-cell response<sup>45,47</sup> and Foxp3 T-reg induction.<sup>43,48</sup> In contrast to this, we have shown that ultra-small OTII-NPs (2-6 nm) are, in part, taken up by DCs following ID injection and are subsequently transported to the local draining LN. Mice deficient in the LN homing receptor CCR7 demonstrated significantly less proliferation in the draining LN, particularly at the high concentration peptide-NP formulation. We therefore hypothesize that the enhancement in the distribution afforded by gold NP conjugation to poorly soluble peptides is, in part, due to enhanced trafficking from the site of injection by DCs, rather than simply by a change to the diffusive properties of the formulation. This finding is of particular interest, as it implies that peptide-NPs could be formulated with a second tolerogenic cargo that could be targeted and co-delivered to skin DCs (rather than LN resident DCs that may be responsible for presentation of ‘naked’ peptide that reaches the LN by diffusion), thus potentially enabling DC function to be modulated prior to migration to the draining LN.

Different affinities of the peptides to their corresponding antigen-specific T-cells resulted in observable differences in the in vivo response to the BDC2.5mimotope, HIP and OTII peptide-bound NP formulations. BDC2.5mimotope peptide, identified by screening a peptide library,<sup>23</sup> has a high affinity to BDC2.5 CD4+ T-cells whereas HIP, a relatively newly-discovered peptide epitope, has been proposed as the natural peptide for the highly diabetogenic BDC2.5 T-cells and thus, in common with many autoantigens, is relatively lower affinity.<sup>22</sup> This relationship was maintained following NP conjugation of the peptides, with HIP-NPs inducing less proliferation than BDC2.5mimotope-NPs at the same peptide dose, thus indicating that NP conjugation to the peptide does not have a detrimental effect on the relative potencies of these auto-antigens.

Previous studies using NPs formulated with an islet autoantigen provide evidence that enhanced expansion of regulatory T-cells in lymphoid organs may translate to a tolerogenic response in diabetes mouse models.<sup>18,19</sup> This was exemplified by an expansion in T regulatory cells and suppression of diabetes development; however neither study delivered antigen by the intradermal route.<sup>18,19</sup> In both of these studies the authors reasoned that NPs would also benefit from a second tolerance-inducing cargo. Indeed, sub-cutaneous delivery of antigen-specific NP formulations, intended to induce tolerance in vivo, has typically used additional anti-inflammatory mediators, such as IL10,<sup>42</sup> rapamycin<sup>34</sup> or TGFβ.<sup>43</sup> HIP-NP studies were therefore extended to explore whether intradermal delivery and enhanced distribution of the peptide to distant LNs could bring about a phenotypic change that is indicative of tolerance in type 1 diabetes i.e. a reduction in IFNγ, a pro-inflammatory cytokine whose levels correlate with disease progression and which is known to enhance the development of type 1 diabetes in the NOD mouse model.<sup>40,41</sup> Down-regulation of this pro-inflammatory mediator IFNγ, three days after administration of HIP-NPs (Figure 7), therefore encourages further investigation of HIP-NP as a therapeutic candidate, potentially a pro-tolerogenic addition to the NP formulation to further enhance regulation.

In this study, NPs were administered via an ID injection using both traditional hypodermic needles and hollow MNs (MicronJet600™). In the mouse model, both methods were able to deliver both peptide and peptide NP formulations into the skin and facilitated comparable in vivo responses. While there are well-recognized differences in murine and human skin, here, both methods of delivery proved equal in their ability to deliver peptide and peptide-NP. Both methods are easily translatable to humans, and peptide and peptide-NP are presented in LNs distant to the site of injection.<sup>9</sup>

In conclusion, this study illustrates the potential value of the intradermal delivery of ultra-small gold NPs for enhanced delivery of lipophilic peptide autoantigens to lymphoid organs and the importance of peptide dose, affinity and solubility on distribution to, and T-cell expansion at, these body sites. Peptide-NP formulations therefore potentially provide a valuable means of targeting poorly soluble peptide epitopes to internal directly inaccessible LNs, such as the pancreatic LN, which may be of particular value in type 1 diabetes tolerisation strategies. Future

516 studies will investigate the clinical utility of this drug delivery  
517 system in immunotherapy.

## Q21 Uncited references

519 30, 44

## 520 Acknowledgments

521 We thank Drs Kathryn Haskins and Thomas Delong for early  
522 information regarding the HIP peptide prior to publication.

## 523 References

524

525 1.. Anderson MS, Bluestone JA. The NOD mouse: a model of immune  
526 dysregulation. *Annu Rev Immunol* 2005;**23**:447-85.

527 2.. Guilliams M, Henri S, Tamoutounour S, Ardouin L, Schwartz-Cornil I,  
528 Dalod M, et al. From skin dendritic cells to a simplified classification of  
529 human and mouse dendritic cell subsets. *Eur J Immunol*  
530 2010;**40**:2089-94.

531 3.. Henri S, Guilliams M, Poulin LF, Tamoutounour S, Ardouin L, Dalod  
532 M, et al. Disentangling the complexity of the skin dendritic cell network.  
533 *Immunol Cell Biol* 2010;**88**:366-75.

534 4.. Romani N, Flacher V, Tripp CH, Sparber F, Ebner S, Stoitzner P.  
535 Targeting skin dendritic cells to improve intradermal vaccination. *Curr*  
536 *Top Microbiol Immunol* 2012;**351**:113-38.

537 5.. Romani N, Thurnher M, Idoyaga J, Steinman RM, Flacher V. Targeting  
538 of antigens to skin dendritic cells: possibilities to enhance vaccine  
539 efficacy. *Immunol Cell Biol* 2010;**88**:424-30.

540 6.. Gupta J, Park SS, Bondy B, Felner EI, Prausnitz MR. Infusion pressure  
541 and pain during microneedle injection into skin of human subjects.  
542 *Biomaterials* 2011;**32**:6823-31.

543 7.. Coulman S, Allender C, Birchall J. Microneedles and other physical  
544 methods for overcoming the stratum corneum barrier for cutaneous gene  
545 therapy. *Crit Rev Ther Drug Carrier Syst* 2006;**23**:205-58.

546 8.. Kochba E, Levin Y, Raz I, Cahn A. Improved insulin pharmacokinetics  
547 using a novel microneedle device for intradermal delivery in patients  
548 with type 2 diabetes. *Diabetes Technol Ther* 2016;**18**:525-31.

549 9.. Levin Y, Kochba E, Kenney R. Clinical evaluation of a novel  
550 microneedle device for intradermal delivery of an influenza vaccine:  
551 are all delivery methods the same? *Vaccine* 2014;**32**:4249-52.

552 10.. Levin Y, Kochba E, Shukarev G, Rusch S, Herrera-Taracena G, van  
553 Damme P. A phase I, open-label, randomized study to compare the  
554 immunogenicity and safety of different administration routes and doses  
555 of virosomal influenza vaccine in elderly. *Vaccine* 2016;**34**:5262-72.

556 11.. Beals CR, Raikar RA, Schaeffer AK, Levin Y, Kochba E, Meyer BK, et  
557 al. Immune response and reactogenicity of intradermal administration  
558 versus subcutaneous administration of varicella-zoster virus vaccine: an  
559 exploratory, randomised, partly blinded trial. *Lancet Infect Dis*  
560 2016;**16**:915-22.

561 12.. Troy SB, Kouliavskaja D, Siik J, Kochba E, Beydoun H, Mirochnitch-  
562 enko O, et al. Comparison of the immunogenicity of various booster  
563 doses of inactivated polio vaccine delivered intradermally versus  
564 intramuscularly to HIV-infected adults. *J Infect Dis* 2015;**211**:1969-76.

565 13.. Anand A, Zaman K, Estivariz CF, Yunus M, Gary HE, Weldon WC, et  
566 al. Early priming with inactivated poliovirus vaccine (IPV) and  
567 intradermal fractional dose IPV administered by a microneedle device:  
568 a randomized controlled trial. *Vaccine* 2015;**33**:6816-22.

569 14.. Levin Y, Kochba E, Hung I, Kenney R. Intradermal vaccination using  
570 the novel microneedle device MicronJet600: past, present, and future.  
571 *Hum Vaccin Immunother* 2015;**11**:991-7.

15.. Fadeel B, Garcia-Bennett AE. Better safe than sorry: understanding the  
572 toxicological properties of inorganic nanoparticles manufactured for  
573 biomedical applications. *Adv Drug Deliv Rev* 2010;**62**:362-74. 574

16.. de Araujo RFJ, de Araujo AA, Pessoa JB, Freire Neto FP, da Silva GR,  
575 Leitao Oliveira AL, et al. Anti-inflammatory, analgesic and anti-tumor  
576 properties of gold nanoparticles. *Pharmacol Rep* 2017;**69**:119-29. 577

17.. Compostella F, Pitirollo O, Silvestri A, Polito L. Glyco-gold  
578 nanoparticles: synthesis and applications. *Beilstein J Org Chem*  
579 2017;**13**:1008-21. 580

18.. A. Yeste, M.C. Takenaka, I.D. Mascanfroni, M. Nadeau, J.E. Kenison,  
581 B. Patel, A.M. Tukpah, J.A. Babon, M. DeNicola, S.C. Kent, D. Pozo,  
582 F.J. Quintana, Tolerogenic nanoparticles inhibit T-cell-mediated  
583 autoimmunity through SOCS2, *Sci Signal*, 9 (2016) ra61. 584

19.. Clemente-Casares X, Blanco J, Ambalavanan P, Yamanouchi J, Singha  
585 S, Fandos C, et al. Expanding antigen-specific regulatory networks to  
586 treat autoimmunity. *Nature* 2016;**530**:434-40. 587

20.. Dul M, Nikolic T, Stefanidou M, McAteer MA, Williams P, Mous J, et  
588 al. Conjugation of a peptide autoantigen to gold nanoparticles for  
589 intradermally administered antigen specific immunotherapy. *Int J*  
590 *Pharm* 2019;**562**:303-12. 591

21.. Katz JD, Wang B, Haskins K, Benoist C, Mathis D. Following a  
592 diabetogenic T-cell from genesis through pathogenesis. *Cell*  
593 1993;**74**:1089-100. 594

22.. Delong T, Wiles TA, Baker RL, Bradley B, Barbour G, Reisdorph R, et  
595 al. Pathogenic CD4 T-cells in type 1 diabetes recognize epitopes formed  
596 by peptide fusion. *Science* 2016;**351**:711-4. 597

23.. V. Judkowski, C. Pinilla, K. Schroder, L. Tucker, N. Sarvetnick, D.B.  
598 Wilson, Identification of MHC class II-restricted peptide ligands,  
599 including a glutamic acid decarboxylase 65 sequence, that stimulate  
600 diabetogenic T-cells from transgenic BDC2.5 nonobese diabetic mice, *J*  
601 *Immunol*, 166 (2001) 908-917. 602

24.. Barnden MJ, Allison J, Heath WR, Carbone FR. Defective TCR  
603 expression in transgenic mice constructed using cDNA-based [agr]- and  
604 [bgr]-chain genes under the control of heterologous regulatory elements.  
605 *Immunol Cell Biol* 1998;**76**:34-40. 606

25.. Forster R, Schubel A, Breitfeld D, Kremmer E, Renner-Muller I, Wolf  
607 E, et al. CCR7 coordinates the primary immune response by establishing  
608 functional microenvironments in secondary lymphoid organs. *Cell*  
609 1999;**99**:23-33. 610

26.. Dul M, Stefanidou M, Porta P, Serve J, O'Mahony C, Malissen B, et al.  
611 Hydrodynamic gene delivery in human skin using a hollow microneedle  
612 device. *J Control Release* 2017;**265**:120-31. 613

27.. Förster R, Davalos-Misslitz AC, Rot A. CCR7 and its ligands: balancing  
614 immunity and tolerance. *Nat Rev Immunol* 2008;**8**:362-71. 615

28.. Zhao X, Coulman SA, Hanna SJ, Wong FS, Dayan CM, Birchall JC.  
616 Formulation of hydrophobic peptides for skin delivery via coated  
617 microneedles. *J Control Release* 2017;**265**:2-13. 618

29.. Suntzeff V, Carruthers C. The water content in the epidermis of mice  
619 undergoing carcinogenesis by methylcholanthrene. *Cancer Res*  
620 1946;**6**:574-7. 621

30.. Steinman RM, Hawiger D, Nussenzweig MC. Tolerogenic dendritic  
622 cells. *Annu Rev Immunol* 2003;**21**:685-711. 623

31.. Merchant B. Gold, the noble metal and the paradoxes of its toxicology.  
624 *Biologicals* 1998;**26**:49-59. 625

32.. Farooq MU, Novosad V, Rozhkova EA, Wali H, Ali A, Fateh AA, et al.  
626 Gold nanoparticles-enabled efficient dual delivery of anticancer  
627 therapeutics to HeLa cells. *Sci Rep* 2018;**8**:2907. 628

33.. Dreaden EC, Austin LA, Mackey MA, El-Sayed MA. Size matters: gold  
629 nanoparticles in targeted cancer drug delivery. *Ther Deliv* 2012;**3**  
630 (4):457-78. 631

34.. Maldonado RA, LaMothe RA, Ferrari JD, Zhang AH, Rossi RJ, Kolte  
632 PN, et al. Polymeric synthetic nanoparticles for the induction of antigen-  
633 specific immunological tolerance. *Proc Natl Acad Sci U S A* 2015;**112**:  
634 E156-E165. 635

35.. Yeste A, Nadeau M, Burns EJ, Weiner HL, Quintana FJ. Nanoparticle-  
636 mediated codelivery of myelin antigen and a tolerogenic small molecule  
637 638

<u>Q21</u>	<p>Uncited references: This section comprises references that occur in the reference list but not in the body of the text. Please position each reference in the text or, alternatively, delete it. Thank you.</p> <div data-bbox="641 273 1128 388" style="border: 1px solid black; padding: 5px; margin: 10px auto; width: fit-content;"><p>Please check this box if you have no corrections to make to the PDF file. <input type="checkbox"/></p></div>
------------	--

Thank you for your assistance.